A DIVERGENCE-FREE VELOCITY RECONSTRUCTION FOR INCOMPRESSIBLE FLOWS

ALEXANDER LINKE

Abstract. In incompressible flows with vanishing normal velocities at the boundary, irrotational forces in the momentum equations should be balanced completely by the pressure gradient. Unfortunately, nearly all available discretization methods for incompressible flows violate this property. The origin of the problem is that discrete velocity approximations of incompressible flows are usually not divergence-free. Hence, the use of divergence-free velocity reconstructions is proposed wherever an L^2 scalar product appears in the discrete variational formulation. The approach is illustrated and applied to a nonconforming MAC-like discretization for unstructured Delaunay grids. It is numerically demonstrated that a divergence-free velocity reconstruction based on the lowest-order Raviart-Thomas element increases the robustness and accuracy of an existing convergent discretization, when irrotational forces appear in the momentum equations.

1. Main result

Accurate and robust numerical simulations of incompressible flows are urgently needed in a wide range of application fields. But, as a matter of fact, nearly all available discretization methods violate a fundamental property of incompressible flows: assuming vanishing normal velocities at the boundary of the underlying domain Ω, a change of the exterior force $\boldsymbol{f} \to \boldsymbol{f} + \nabla\psi$ in the momentum balance equations should change the flow by $(\boldsymbol{u}, p) \to (\boldsymbol{u}, p + \psi)$ [2]. In other words, the flow should not be affected at all, and the additional irrotional force $\nabla\psi$ should be balanced completely by the pressure gradient. The origin of the problem lies in the discretization of the exterior force term $\int_\Omega \boldsymbol{f}\cdot\boldsymbol{v}\,dx$ in a variational formulation. Assuming that we are able to decompose the exterior force $\boldsymbol{f} \in L^2(\Omega)^d$ by a Helmholtz decomposition into a divergence-free part $\boldsymbol{w}$ and an irrotational part $\nabla\phi$, i.e., $\boldsymbol{f} = \boldsymbol{w}+\nabla\phi$, and assuming vanishing normal velocities for the divergence-free velocity $\boldsymbol{v}$, we would obtain $\int_\Omega \boldsymbol{f}\cdot\boldsymbol{v}dx = \int_\Omega \boldsymbol{w}\cdot\boldsymbol{v}dx$, since irrotational and divergence-free fields are orthogonal in the L^2 scalar product. But unfortunately, the Helmholtz decomposition of the exterior force $\boldsymbol{f}$ is difficult to obtain in a discrete setting, and the failure of most discretization schemes w.r.t. $\boldsymbol{f} \to \boldsymbol{f} + \nabla\psi \not\Rightarrow (\boldsymbol{u}, p) \to (\boldsymbol{u}, p + \psi)$ results in the simple fact that discretely divergence-free velocities $\boldsymbol{v}_h$ in conforming discretizations or, correspondingly, reconstructions of discretely divergence-free velocities in nonconforming discretizations are generally not divergence-free, i.e., their distributional divergence is either not in $L^2(\Omega)$ or does not vanish. Therefore, we obtain for the discretization of the exterior force $\int_\Omega \boldsymbol{f}\cdot\boldsymbol{v}_h dx \neq \int_\Omega \boldsymbol{w}\cdot\boldsymbol{v}_h dx$. Indeed, in many coupled flow situations the contribution of the irrotational part $\nabla\phi$ in $\boldsymbol{f}$ can be much larger than the divergence-free part [2], and the numerical computations of such problems are spoiled by large numerical errors. Moreover, also the nonlinear convection term $(\boldsymbol{u}\cdot\nabla)\boldsymbol{u}$, the Coriolis term $2\boldsymbol{\Omega}\times\boldsymbol{u}$ or the nonlinear convection term $(\nabla\times\boldsymbol{u})\times\boldsymbol{u}$ in the rotational formulation of the Navier-Stokes equations may have a large irrotational part in an incompressible flow, exciting exactly the same kind of numerical errors.

The numerical inaccuracies emanating from $\boldsymbol{f} \to \boldsymbol{f} + \nabla\psi \not\Rightarrow (\boldsymbol{u}, p) \to (\boldsymbol{u}, p + \psi)$ are well-experienced in the scientific community and several techniques have been proposed, in order to circumvent the problem, most prominently the so-called grad-div stabilization in conforming mixed finite elements. Other approaches solve auxiliary problems, in order to overcome the problem. But the solution of auxiliary problems is expensive, and mitigates the problem only. Although there are few really divergence-free methods, like the Scott-Vogelius element or some divergence-free Discontinuous Galerkin methods, they are expensive and rarely used in practice.

Instead, in this short note it is proposed to start from existing convergent discretizations and to enhance their numerical accuray by introducing appropriate divergence-free reconstructions. The divergence-free reconstruction has to enter the discrete variational formulation wherever a vectorial

L^2 scalar product with a velocity test function appears. Hence, e.g., the exterior force $\boldsymbol{f}$ has to be discretized in a discrete weak formulation as $\int_\Omega \boldsymbol{f}\cdot\boldsymbol{R}_h(\boldsymbol{v}_h)dx$. The reconstruction $\boldsymbol{R}_h$ has to map discretely divergence-free velocities $\boldsymbol{v}_h$ with vanishing normal velocities onto divergence-free vector fields in $\{\boldsymbol{v}\in L^2(\Omega)^d : \nabla\cdot\boldsymbol{v}=0 \wedge \boldsymbol{v}\cdot\boldsymbol{n}=0\}$. In this note, this approach is demonstrated for a extension of the classical MAC scheme to unstructured Delaunay grids[1, 3]. Here, the discrete velocities are the normal velocity components orthogonal to the triangle edges, and the triangles of the mesh are the control volumes for the discrete divergence operator. The classical $H(\mathrm{div})$-conforming Raviart-Thomas finite element of lowest order is applied, in order to lift the discrete normal velocity components to a full velocity $\boldsymbol{R}_h(v_h)\in H(\mathrm{div})$. As an illustration, we present numerical results for the incompressible Stokes equations $-\nu\Delta\boldsymbol{u}+\nabla p=\boldsymbol{f}, \nabla\cdot\boldsymbol{u}=0$. The problem is posed on the domain $\Omega=[0,1]^2$ and has homogeneous Dirichlet boundary conditions. In the numerical example, the continuous solution $\boldsymbol{u}=(2(x-1)^2x^2(y-1)y(2y-1), -2(2x-1)(x-1)x(y-1)^2y^2)^T$, $p=x^3+y^3-\frac{1}{2}$ is approximated by two different finite volume schemes that are described below. The computations are done for two different viscosities $\nu\in\{1,10^{-7}\}$. The forcing is given by $\boldsymbol{f}=-\nu\Delta\boldsymbol{u}+\nabla p$. Therefore, the smaller is ν, the more dominant is the irrotational part of $\boldsymbol{f}$ in the sense of the Helmholtz decomposition. From Table 1 we indeed recognize that the new scheme

mesh size	$\nu=1$: $\|\boldsymbol{I}_h\boldsymbol{u}-\boldsymbol{u}_h\|_0$	$\nu=1$: $\|\boldsymbol{I}_h\boldsymbol{u}-\boldsymbol{u}_{h,\mathrm{divfree}}\|_0$	$\nu=10^{-7}$: $\|\boldsymbol{I}_h\boldsymbol{u}-\boldsymbol{u}_h\|_0$	$\nu=10^{-7}$: $\|\boldsymbol{I}_h\boldsymbol{u}-\boldsymbol{u}_{h,\mathrm{divfree}}\|_0$
$\frac{1}{4}$	$3.28\cdot10^{-3}$	$1.97\cdot10^{-3}$	$9.86\cdot10^{2}$	$1.97\cdot10^{-3}$
$\frac{1}{8}$	$8.80\cdot10^{-4}$	$6.99\cdot10^{-4}$	$1.36\cdot10^{2}$	$6.99\cdot10^{-4}$
$\frac{1}{16}$	$2.54\cdot10^{-4}$	$2.19\cdot10^{-4}$	$3.49\cdot10^{1}$	$2.19\cdot10^{-4}$
$\frac{1}{32}$	$7.49\cdot10^{-5}$	$6.78\cdot10^{-5}$	$5.96\cdot10^{0}$	$6.78\cdot10^{-5}$

TABLE 1. Numerical comparison of two finite volume schemes for the incompressible Stokes equations. In columns 2 and 4, the results for the unmodified scheme are presented. In columns 3 and 5, the results of the new scheme with a divergence-free reconstruction of the velocity are given. The results are measured in the L^2 norm of the velocity and show the differences between an interpolation of the exact velocity $\boldsymbol{I}_h\boldsymbol{u}$ and the discrete solutions $\boldsymbol{u}_h$ and $\boldsymbol{u}_{h,\mathrm{divfree}}$.

with a divergence-free reconstruction of the discrete velocity performs better for small viscosities ν. Since this scheme fulfills the property $\boldsymbol{f}\to\boldsymbol{f}+\nabla\psi \Rightarrow (\boldsymbol{u},p)\to(\boldsymbol{u},p+\psi)$ in a discrete sense, the results for the discrete velocity are completely independent of ν (columns 3 and 5), i.e., the results are independent of the irrotational part of $\boldsymbol{f}$. Since the unmodified scheme (columns 2 and 4) does not fulfill this property, the numerical results are different for different values of ν. For small values of ν, the unmodified scheme without a divergence-free reconstruction performs poorly (column 4), see also Picture 1.

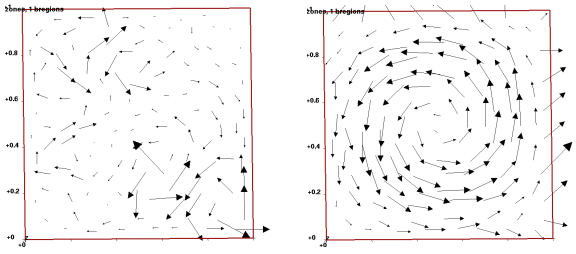

FIGURE 1. Numerical results on the mesh with mesh size $\frac{1}{8}$ for the two finite volume schemes, $\nu=10^{-7}$. Reconstructions of the discrete velocity are presented for the unmodified scheme (left) and for the scheme with divergence-free reconstruction (right)

2. Definition of the scheme

Definition 2.1 (Acute triangulation of Ω)**.** *Assuming that $\Omega \subset \mathbb{R}^2$ is a polygonal bounded and connected domain, an acute triangular mesh of Ω is defined by $\mathcal{M} = (\mathcal{V}, \mathcal{E}, \mathcal{T})$ such that:*

1. *The set $\mathcal{T}$ is a finite set of disjoint (open) triangles such that $\bigcup_{T\in\mathcal{T}} \overline{T} = \overline{\Omega}$. We denote by $h_{\mathcal{M}}$ the largest diameter of all triangles. For all $T \in \mathcal{T}$ the circumcenters $\boldsymbol{x}_T$ of T are located within T.*
2. *The set $\mathcal{V}$ consists of the vertices of all the triangles. For all $\boldsymbol{y} \in \mathcal{V}$, we denote by $V_{\boldsymbol{y}}$ the Voronoi box around the vertex $\boldsymbol{y} \in \mathcal{V}$, defined as $V_{\boldsymbol{y}} = \{\boldsymbol{x} \in \Omega, |\boldsymbol{x} - \boldsymbol{y}| < |\boldsymbol{x} - \boldsymbol{y'}| \text{ for all } \boldsymbol{y'} \in \mathcal{V}, \boldsymbol{y'} \neq \boldsymbol{y}\}$.*
3. *The set $\mathcal{E}$ consists of all the edges of the triangles. We denote by $\boldsymbol{x}_\sigma$ the midpoint of σ.*

For every edge $\sigma \in \mathcal{E}$, we define a fixed orientation, which is given by an unit vector $\boldsymbol{t}_\sigma$ parallel to σ, and we define $\boldsymbol{n}_\sigma$ as the normal vector to σ, obtained from $\boldsymbol{t}_\sigma$ by a rotation with angle $\pi/2$ in the counterclockwise sense. For every $T \in \mathcal{T}$, we denote by $\mathcal{E}_T$ the set of edges of the triangle

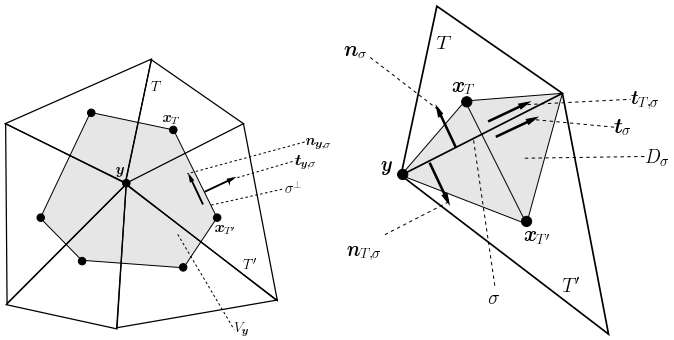

FIGURE 2. Notations for the mesh: Left: the Voronoi box associated to a vertex. Right: Zoom on a diamond.

T. $\boldsymbol{t}_{T\sigma}$ denotes the unit vector parallel to σ oriented in the counterclockwise sense around T. By $\boldsymbol{n}_{T\sigma}$ we denote the unit vector normal to σ and outward to T, and by $D_{T,\sigma}$ the cone with basis σ and vertex $\boldsymbol{x}_T$. Analogously, $\mathcal{E}_{\boldsymbol{y}}$ describes all the edges adjacent to the vertex $\boldsymbol{y} \in \mathcal{V}$. By $V_{\boldsymbol{y}}$ we denote the Voronoi box around the vertex $\boldsymbol{y} \in \mathcal{V}$. By $\sigma^\perp$ we denote the Voronoi face perpendicular to σ. By $\boldsymbol{t}_{\boldsymbol{y}\sigma}$ we denote a unit vector tangential to $\boldsymbol{t}_\sigma$, but pointing outward w.r.t. the Voronoi box $V_{\boldsymbol{y}}$, and $\boldsymbol{n}_{\boldsymbol{y}\sigma}$ denotes its counterclockwise rotation. Last but not least, we denote by $\boldsymbol{x}_{T,\sigma}$ the vertex of triangle T which is opposite to the edge $\sigma \in \mathcal{E}_T$.

Now the discretization is given as follows. The discrete pressure space is denoted by $X_{\mathcal{T}} = \mathbb{R}^{\mathcal{T}}$. It represents the pressures at the circumcenters of the elements. For the velocity space we use the notations $X_{\mathcal{E}}$ and $\dot{X}_{\mathcal{E}}$. $X_{\mathcal{E}}$ represents the space of *normal velocities* approximating the continuous velocity $\boldsymbol{u} \cdot \boldsymbol{n}_\sigma$. $\dot{X}_{\mathcal{E}}$ is a subspace of $X_{\mathcal{E}}$ with vanishing normal velocities at the boundary $\partial\Omega$. The normal velocities of the space $X_{\mathcal{E}}$ are located at the midpoints of all the Voronoi faces $\sigma^\perp$. We define $\operatorname{rot}_{\boldsymbol{y}} v = \frac{1}{|V_{\boldsymbol{y}}|} \sum_{\sigma\in\mathcal{E}_{\boldsymbol{y}}} |\sigma^\perp| v_\sigma \boldsymbol{n}_\sigma \cdot \boldsymbol{n}_{\boldsymbol{y}\sigma}$ for all $v \in X_{\mathcal{E}}$, $\boldsymbol{y} \in \mathcal{V}$ and $\operatorname{div}_T v = \frac{1}{|T|} \sum_{\sigma\in\mathcal{E}_T} |\sigma| v_\sigma \boldsymbol{n}_\sigma \cdot \boldsymbol{n}_{T\sigma}$ for all $v \in X_{\mathcal{E}}$, $T \in \mathcal{T}$, see again Figure 2 for the notations, and write: find $(u, p_{\mathcal{T}}) \in \dot{X}_{\mathcal{E}} \times X_{\mathcal{T}}$ such that

$$\sum_{\boldsymbol{y}\in\mathcal{V}} |V_{\boldsymbol{y}}| \nu \operatorname{rot}_{\boldsymbol{y}} u \operatorname{rot}_{\boldsymbol{y}} w - \sum_{T\in\mathcal{T}} |T| p_T \operatorname{div}_T w = \sum_{\sigma\in\mathcal{E}} 2 w_\sigma \int_{D_\sigma} \boldsymbol{f} \cdot \boldsymbol{n}_\sigma \mathrm{d}\boldsymbol{x}, \ \forall w \in \dot{X}_{\mathcal{E}} \tag{1}$$

$$\operatorname{div}_T u = 0, \ \forall T \in \mathcal{T}.$$

Assuming $\boldsymbol{f} \in \mathbb{R}(\Omega)^2$, the convergence of this scheme was proven in [1]. In the new, second scheme, the discrete differential operators remain unchanged, and only the right hand side is replaced by a divergence-conforming Raviart-Thomas reconstruction, i.e.,

$$\sum_{T\in\mathcal{T}} \sum_{\sigma\in\mathcal{E}_T} \int_T \boldsymbol{f} \cdot \left(w_\sigma (-\boldsymbol{n}_{T\sigma} \cdot \boldsymbol{n}_\sigma) \frac{\boldsymbol{x} - \boldsymbol{x}_{T,\sigma}}{|(\boldsymbol{x}_\sigma - \boldsymbol{x}_{T,\sigma}) \cdot \boldsymbol{n}_\sigma|} \right) \mathrm{d}\boldsymbol{x}.$$

References

[1] R. Eymard, J. Fuhrmann, A. Linke: *MAC schemes on triangular Delaunay meshes*. WIAS-Preprint 1654, Berlin, 2011, submitted.
[2] K. Galvin, A. Linke, L. G. Rebholz, N. E. Wilson: *Stabilizing poor mass conservation in incompressible flow problems with large irrotational forcing and application to thermal convection*. Comput. Methods Appl. Mech. Engrg. 237–240, pp. 166–176, 2012.
[3] R. A. Nicolaides, T. A. Porsching, C. A. Hall. *Covolume methods in computational fluid dynamics*, in: M. Hafez, K. Oshma (Eds.), Computation Fluid Dynamics Review, pp. 279-299. John Wiley and Sons, New York, 1995.

Free University Berlin, Department of Mathematics and Computer science, Arnimallee 6, 14195 Berlin, alexlinke@zedat.fu-berlin.de